ELSEVIER

Catalysis Today 62 (2000) 379–388

CATALYSIS TODAY

www.elsevier.com/locate/cattod

Catalytic wet oxidation of phenol over $Pt_xAg_{1-x}MnO_2/CeO_2$ catalysts☆

S. Hamoudi[a], A. Sayari[a], K. Belkacemi[b], L. Bonneviot[c], F. Larachi[a,*]

[a] *Department of Chemical Engineering & CERPIC, Laval University, Laval, Que., Canada G1K 7P4*
[b] *Department of Food Science & Nutrition, Laval University, Laval, Que., Canada G1K 7P4*
[c] *Department of Chemistry & CERPIC, Laval University, Laval, Que., Canada G1K 7P4*

Abstract

Catalytic wet oxidation reactions of aqueous phenol over unpromoted, base- and noble-metal promoted MnO_2/CeO_2 catalysts were carried out under mild conditions (80–130°C, 0.5 MPa O_2) in a batch slurry reactor. Even though the catalyst-mediated oxidation was very effective in destroying phenol, only a moderate selectivity toward complete mineralization into CO_2 and H_2O was attained due to parallel formation of deactivating carbonaceous deposits. Promotion of the mixed-oxide catalysts with platinum and/or silver enhanced the mineralization selectivity and reduced appreciably the amount of deposits.

Keywords: Catalytic wet oxidation; Noble metal promotion; Cerium and manganese oxides; Phenol oxidation

1. Introduction

In recent years, the problem of disposing of wastewaters containing toxic organic pollutants has become increasingly acute due to the tightening of environmental regulations. Catalytic wet oxidation (CWO) using heterogeneous catalysts is being developed as a powerful technique for the treatment of dilute aqueous wastestreams contaminated by a variety of organic pollutants such as phenols. Catalysts are used to accomplish the oxidative treatment under much milder conditions (typically 80–150°C; 0.1–2 MPa O_2) than the non-catalytic route [1,2]. While ranging in effectiveness and life time, solid catalysts may be preferred to their homogeneous counterparts as they offer a number of advantages including easy recovery, regeneration and reuse of the catalysts, as well as easy set-up for continuous operations. A large variety of solid catalysts including supported and unsupported metal oxides and noble metals supported on metal oxides or on acid-proof supports, have been tested in the oxidation of water pollutants. While the high activity in CWO of some of them, e.g. Ru/CeO_2, MnO_2/CeO_2, Co_3O_4/Bi_2O_3, $CuO–ZnO/Al_2O_3$ has been demonstrated [2–4], their longevity, and more particularly their resistance to deactivation by carbonaceous deposits has not been thoroughly addressed in the literature.

Previous work in our laboratory on CWO of phenol [5–8] over unpromoted MnO_2/CeO_2 catalyst revealed that even when complete removal of organic carbon from the solution was achieved, an important fraction of the initial carbon was transformed into a polymeric material strongly adsorbed on the catalyst surface.

☆ Paper presented in session [310]: Environmental Catalysis II, AIChE meeting, Dallas, 10/30-11/5 1999.

* Corresponding author. Tel.: +1-418-656-3566; fax: +1-418-656-5993.
E-mail address: flarachi@gch.ulaval.ca (F. Larachi).

0920-5861/00/$ – see front matter
PII: S0920-5861(00)00439-9

Nomenclature

[A]	phenol carbon lump, mol C m^{-3} solution
[B]	carbon concentration of dissolved organic intermediate lump, mol C m^{-3} solution
[C]	carbon concentration of fully mineralised carbon lump, mol C m^{-3} solution
[C_S]	carbon concentration of carbon deposited on the catalyst, mol C m^{-3} solution
K, K'	adsorption equilibrium constants, m^3 mol^{-1}
k, k', $\tilde{k}$	rate constants, mol kg^{-1} min^{-1} or min^{-1}
[m_c]	catalyst loading, kg m^{-3}
S_M	mineralization selectivity
t	time, min
T	temperature, °C or K
TOC	total organic carbon, g C l^{-1} or mol C l^{-1}
[W]	carbon concentration of carbonaceous deposit lump, mol C m^{-3} solution
α	catalyst activity

This deposit was shown to be responsible for catalyst deactivation via physical blockage of active sites [7]. On the other hand, the use of a noble-metal containing catalyst such as platinum over alumina generated lesser build-ups of deposits [5]. However, due to its weaker activity, longer reaction times and higher oxidation temperatures were required [5] to attain phenol conversions comparable to those with MnO_2/CeO_2. Platinum, as a noble metal, very likely catalyzes the C–C bond rupture within the organic molecules, while simultaneously, it prevents extensive polymerization of the reactive intermediate radicals that form in the course of CWO [6]. Silver supported on metal oxides has also proved efficient in gas-phase catalytic combustion of light hydrocarbons, volatile organic compounds, carbon monoxide, methane, etc. [9,10]. Oxygen adsorption on Ag is known to lead to oxygen species responsible for both partial and deep oxidation [10]. This latter property is of particular interest for liquid-phase CWO applications. The motivation of using silver alone or in conjunction with a noble metal, such as platinum, is three-fold. First, silver as a base metal may be a cheaper alternative to precious metals, and is thus economically more attractive for the treatment of large bodies of liquids ending up as "zero-added-value" decontaminated waters. Second, as single base-metal containing catalysts cannot rival a precious metal-containing catalyst, improvement in catalyst activity by combining a base metal with a precious metal may constitute a good trade-off between cost and activity. Third, (co)promoting MnO_2/CeO_2 with Pt, Ag or Pt–Ag is expected to suppress or at least to diminish the formation of carbonaceous deposits by side reactions.

In this work, we concentrated our efforts on the synthesis and the characterization of several fresh and spent $Pt_xAg_{1-x}MnO_2CeO_2$ catalysts for the CWO of model aqueous phenol solutions. The promotion by base and noble metals of MnO_2/CeO_2 was explored as an alternative to the use of the pure composite oxides to inhibit the polymerization side reactions, improve the mineralization selectivity of CWO and ultimately prolong the catalyst longevity. As far as catalyst metallic doping is concerned, impregnation (or incipient wetness) and ion exchange wet preparation methodologies are the known recipes in use for promoting CWO catalysts. Both methodologies will be explored and their performances compared in this study.

2. Experimental

2.1. Materials

Phenol (99 + % purity) purchased from BDH Co. was used without further purification. Purified acetic anhydride and pyridine used for phenol esterification were analytical grade reagents. Fisher Scientific Co. supplied naphthalene used as an internal standard in GC analyses.

The MnO_2/CeO_2 catalyst (molar ratio = 7/3) was synthesized by coprecipitation of $MnCl_2$ (Fisher Scientific Co.) and $CeCl_3$ (Sigma Chemicals Co.) [11]. The precipitate was filtered, washed and dried overnight at 100°C. Then, it was calcined under flowing air at 350°C for 3 h.

Platinum was loaded on the MnO_2/CeO_2 support via impregnation (incipient wetness) and ion exchange using an aqueous solution of a chlorine-containing

precursor, H_2PtCl_6, and a chlorine-free precursor, $K_2Pt(CN)_6$ (Aldrich Chemicals Co.). The platinum nominal content was varied, from 0.1 to 2 wt.% and from 0.4 to 4 wt.% for ion exchanged and impregnated samples, respectively. Subsequently, the catalysts were calcined in an air flow at 350°C, cooled to room temperature, then exposed to flowing hydrogen (30 ml min^{-1}) at 250°C for 2 h to reduce platinum to its metallic state.

The silver containing single and bimetallic catalysts were prepared by impregnation from aqueous solutions of $AgNO_3$ (Aldrich Chemicals Co.) and $K_2Pt(CN)_6$. Instead of H_2PtCl_6, the non-chlorinated platinum salt precursor was used to prevent precipitation of silver chloride. The silver-containing samples were calcined in flowing air at 350°C for 3 h but not reduced. The metal loading design of Ag and Pt in promoted MnO_2/CeO_2 samples is summarized in Fig. 1.

2.2. Catalyst characterization

The catalysts were characterized by N_2 physical adsorption at 77 K using an Omnisorp 100 sorption instrument from Coulter. Their surface area was determined using the BET (Brunauer–Emmett–Teller) model. XRD patterns were obtained on Siemens D5000 powder diffractometer using Co Kα radiation ($\lambda = 1.789$ Å).

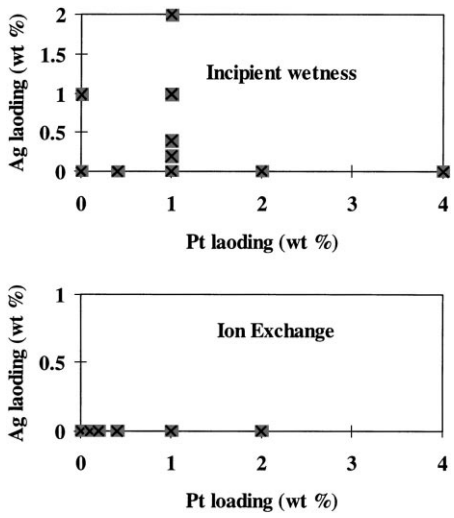

Fig. 1. Metal loading design of catalyst formulations.

The reducibility of the base (and noble) metal-promoted catalysts was investigated by temperature programmed reduction (TPR) using an Altamira AMI1 instrument. In a typical TPR run, 60–100 mg of dehydrated catalyst was loaded in a U-shaped quartz microreactor. Dilute hydrogen stream (10% v/v H_2/Ar) at a constant flow rate of 30 cm^3 min^{-1} was used, and the sample temperature was increased from room temperature to 650°C at 10°C min^{-1} heating rate. Analysis of the microreactor outlet gas was performed by thermal conductivity and mass spectrometry.

The carbon content of the carbonaceous deposits on the catalyst surface was quantified by CHN elemental analysis (Carlo Erba, Model 1106). Burn-off profiles of these deposits were obtained by temperature programmed oxidation (TPO) using the Altamira AMI1 instrument. Additional experimental details may be found elsewhere [5].

2.3. Reaction procedure and analytical methods

Phenol was oxidized in a 300 ml stainless steel high-pressure Parr agitated autoclave reactor (model 4842, Parr Instrument, Inc.) in the temperature range 80–130°C using a catalyst load of 5 g l^{-1} under 0.5 MPa O_2 pressure. This partial pressure corresponded to an oxygen/phenol stoichiometric ratio of ca. 7 (assuming full conversion of phenol into carbon dioxide and water). The autoclave was first charged with 96 ml of pure water and the catalyst. Once the system had stabilized at the desired reaction conditions, a concentrated phenol solution (4 ml, 25 g l^{-1}) was added. For this purpose, the autoclave was equipped with a reagent injection device connected to a secondary oxygen inlet.

At preset reaction times, aliquots of the solution were withdrawn and analyzed for: (i) total organic carbon (*TOC*) using a combustion/non-dispersive infrared gas analyzer (Shimadzu 5050 *TOC* analyzer), and (ii) residual phenol concentration. The latter was analyzed after derivatization using a Hewlett-Packard gas chromatograph (HP5890 series II plus) equipped with a mass selective detector (MSD model HP5972). For gas chromatography analysis, the sample volume injected was 1 μl and naphthalene dissolved in ethylacetate was used as an internal standard. A HP-5MS 30 m × 0.25 mm i.d. capillary column was used in

Table 1
Physical characteristics of representative catalyst compositions

Catalyst	S_{BET} ($m^2\,g^{-1}$)	Pore volume ($ml\,g^{-1}$)	Average pore diameter (nm)
MnO_2/CeO_2	107	0.405	0.51
Pt(1%)–MnO_2/CeO_2 [a]	91	0.329	0.51
Pt(1%)–MnO_2/CeO_2 [b]	84	0.302	0.50
Ag(1%)–MnO_2/CeO_2	93	0.334	0.51
Pt–Ag(1–1%)–MnO_2/CeO_2	76	0.273	0.52

[a] Impregnated.
[b] Ion exchanged.

temperature-programmed mode, and helium carrier (ultrahigh purity) at a flow rate of $1\,ml\,min^{-1}$ was the sweeping gas. The oven temperature was held at 50°C for the first 2 min, then raised to 120°C at a rate of $5°C\,min^{-1}$. The temperatures of the injector and GC-MSD interface were 250 and 280°C, respectively.

3. Results

3.1. Catalyst characterization

Table 1 summarizes the observed physical properties of representative catalysts with the two types of promoting metals and metal loadings. As shown, irrespective of the metal loading technique, the BET surface area and the pore volumes of the promoted MnO_2/CeO_2 were lower than those corresponding to the unpromoted mixed oxide. In contrast, the pore size remained unchanged at ca. 0.5 nm for all the samples. Fig. 2. shows the obtained diffractogramms for the representative catalyst compositions of Table 1. The diffraction pattern of MnO_2/CeO_2 (Fig. 2a) revealed a low degree of crystallinity with some diffraction lines around 30 and 40°, in agreement with the observations by Imamura et al. [12]. In the case of the single (Pt– or Ag–) or bimetallic (Pt–Ag–) MnO_2/CeO_2, i.e. Fig. 2b–e, the diffraction patterns did not show

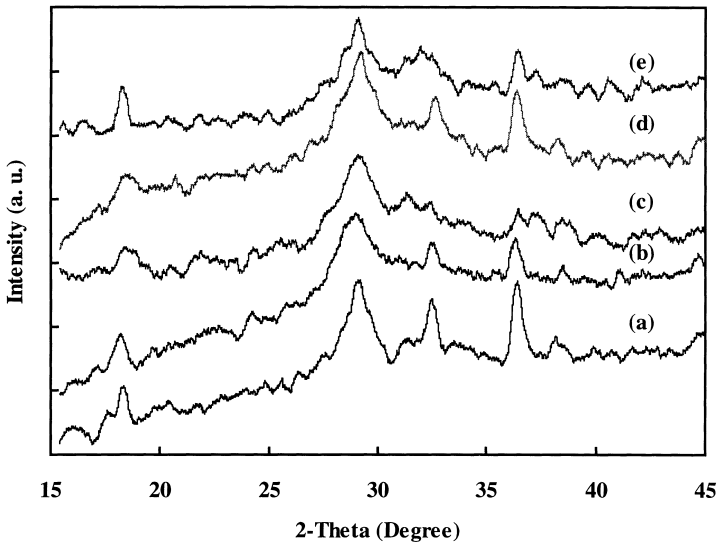

Fig. 2. XRD patterns of (a) MnO_2/CeO_2; (b) Pt–MnO_2/CeO_2 (impregnated); (c) Pt–MnO_2/CeO_2 (ion exchanged); (d) Ag–MnO_2/CeO_2; (e) Pt–Ag–MnO_2/CeO_2.

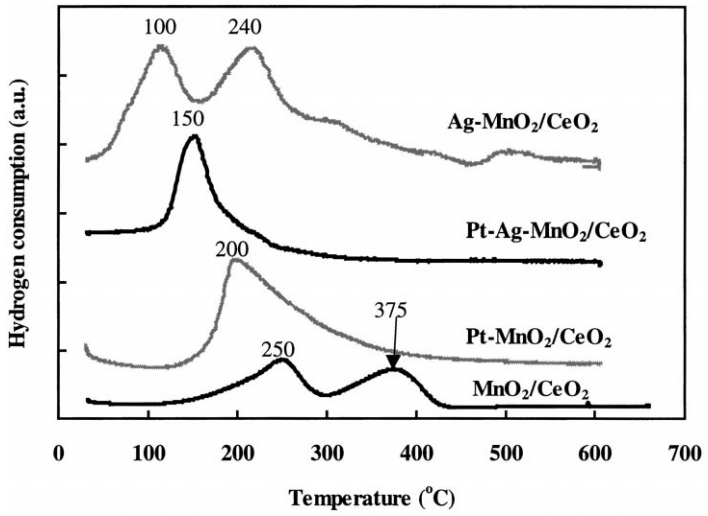

Fig. 3. TPR profiles of MnO_2/CeO_2 and M–MnO_2/CeO_2 (M: Pt and/or Ag).

dramatic alterations. The absence of additional peaks characteristic of Pt and/or Ag oxides suggests that the promoting metals have a high degree of dispersion on the mixed oxide surface.

The reducibility of unpromoted and metal-promoted MnO_2/CeO_2 mixed oxide catalysts was investigated by means of the TPR technique. The reduction profiles of the bare composite oxides, the mono-metallic and bimetallic promoted oxides are presented in Fig. 3. The unpromoted catalyst exhibited two reduction peaks located at 250 and 375°C attributed to the reduction of Mn and Ce oxides, respectively. Interestingly, for the Pt(1 wt.%)–MnO_2/CeO_2 and Pt–Ag(1–1 wt.%)–MnO_2/CeO_2 catalysts, the peaks merged into one peak and shifted left-wise to lower temperatures to about 200 and 150°C, respectively. This finding supports the existence of metal–metal as well as metal-support interactions which are considered key factors in controlling the catalyst properties [13–15]. These interactions are likely strengthened by the presence of ceria that induces either the well-known spillover of hydrogen from Pt and/or Ag to CeO_2, or an increase in the oxygen mobility within CeO_2 [13,16,17]. In the case of Ag(1 wt.%)–MnO_2/CeO_2, two reduction peaks at 100 and 240°C were observed. It is worth mentioning that the lowest reduction peak at 100°C coincides with the range of CWO temperatures explored in this study. Unlikely to be a simple coincidence, this may be at the origin of the superior performance obtained with this catalyst formulation as to be shown later.

The shifts toward lower reduction temperatures clearly demonstrate the improvement of the low temperature redox properties of the MnO_2/CeO_2 catalyst by promotion with platinum and/or silver.

3.2. CWO over unpromoted MnO_2/CeO_2

Typical phenol degradation profiles over MnO_2/CeO_2 are depicted in Fig. 4a and b as phenolic carbon conversion and solid carbon buildup on the catalyst versus time, respectively. The reaction was carried out in the temperature range 80–130°C under constant oxygen partial pressure (0.5 MPa) using $1\,g\,l^{-1}$ initial phenol concentration and $5\,g\,l^{-1}$ catalyst loading. While complete removal of the pollutant from water was achieved within 30 min at 130°C (phenol conversion 100%), at 80°C, more than 120 min were required to reach comparable results (phenol conversion = 98%). Despite the remarkable performance of the MnO_2/CeO_2 catalyst to remove phenol from water, most of the converted pollutant transformed into carbonaceous deposits on the catalyst surface as illustrated in Fig. 4b. Regardless of the temperature, the pure mixed oxide catalyst exhibited a poor performance toward complete mineralization

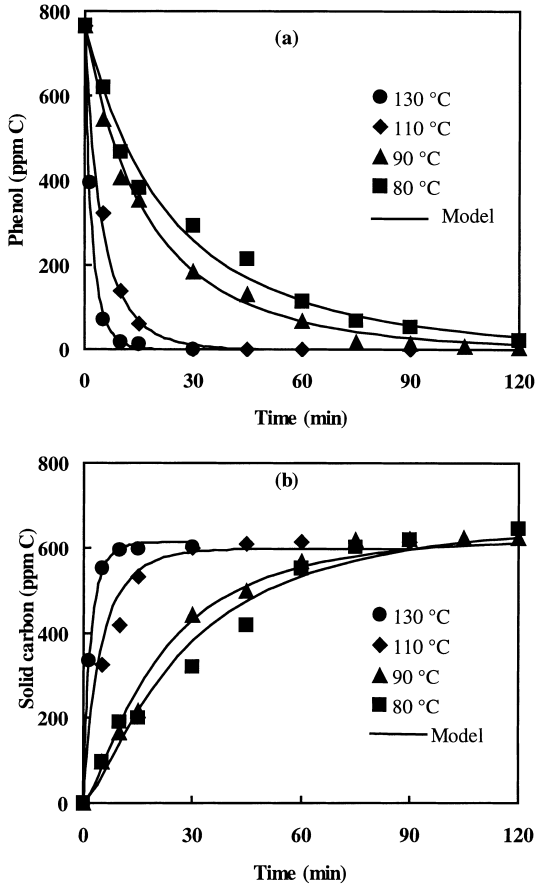

Fig. 4. Effect of temperature on (a) phenol conversion, and (b) catalyst carbon content during CWO over MnO_2/CeO_2 (0.5 MPa O_2 pressure, 1 g l^{-1} phenol initial concentration, 5 g l^{-1} catalyst loading). Lines show Four-Lump LHHW kinetic model predictions.

of phenol. Furthermore, the carbonaceous deposits were shown to induce catalyst deactivation as recycled non-regenerated catalysts exhibited a progressive loss in activity [6].

As shown in an earlier work [7], experimental data for phenol CWO over MnO_2/CeO_2 were described by means of a four-lump Langmuir–Hinshelwood–Hougen–Watson (LHHW) kinetic model taking into account the catalyst activity-decline due to the formation and accumulation of the carbonaceous materials over the catalyst surface. These four lumps were phenol (A), dissolved phenol oxidation reaction intermediates (B), solid carbon (W), and the products (total inorganic carbon), i.e. CO_2 (C). The multiple deactivation-reaction network represented mechanistically by a sequence of LHHW elementary steps is shown in Fig. 5.

The final model equations drawn from this scheme were based on the following assumptions.

1. The surface reaction steps of chemisorbed phenol and its daughter by-products (B*) are rate controlling compared to their adsorption and desorption steps.
2. Catalyst deactivation occurs via site coverage over single-type sites.
3. Deactivation occurs via parallel fouling reactions, and an identical deposit is formed by the two main reactions of the network.
4. The foulant adsorbs irreversibly on the catalyst and its rate of desorption is negligible.
5. The deactivation function is defined as the fraction of active sites remaining active [12].

For the sake of conciseness, the different mathematical developments leading to the final rate equations

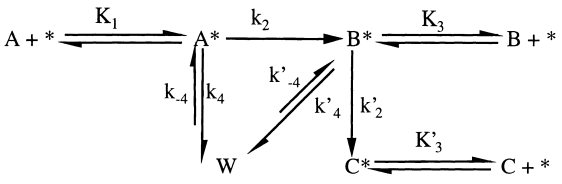

Lump A: Reactant
Lump B: Dissolved intermediates
Lump C: Gaseous products
Lump W: Carbonaceous deposits

Fig. 5. Proposed reaction scheme for phenol CWO with formation of carbonaceous deposits.

describing the time profiles for the four lumps implied in the reaction scheme are not reported here (see ref. [7]). The obtained differential and algebraic system giving the time evolution of the four lumps and the catalyst activity decline is:

$$-\frac{\mathrm{d[A]}}{\mathrm{d}t} = \frac{\tilde{k}_2 K_1 [\mathrm{m_c}][\mathrm{A}]\alpha}{1 + K_1[\mathrm{A}] + K_3[\mathrm{B}] + K_3'[\mathrm{C}]} \quad (1)$$

$$\frac{\mathrm{d[B]}}{\mathrm{d}t} = \frac{[\mathrm{m_c}](\tilde{k}_2 K_1[\mathrm{A}] - \tilde{k}_2 K_3[\mathrm{B}])\alpha}{1 + K_1[\mathrm{A}] + K_3[\mathrm{B}] + K_3'[\mathrm{C}]} \quad (2)$$

$$-\frac{\mathrm{d}\alpha}{\mathrm{d}t} = \frac{(k_4 K_1[\mathrm{A}] + k_4' K_3[\mathrm{B}])\alpha}{1 + K_1[\mathrm{A}] + K_3[\mathrm{B}] + K_3'[\mathrm{C}]} \quad (3)$$

$$[\mathrm{C}] = [\mathrm{A}]_0 - [\mathrm{A}] - [\mathrm{B}] - [\mathrm{W}]_\infty(1 - \alpha) \quad (4)$$

$$[\mathrm{W}] = \frac{\%\mathrm{C}}{12}[\mathrm{m_c}] \quad (5)$$

subject to the following initial conditions at $t = 0$: $\alpha = 1$; $[\mathrm{A}] = [\mathrm{A}]_0$; $[\mathrm{B}] = [\mathrm{C}] = 0$.

For a deactivation occurring by site coverage over single-type sites, the deactivation function, α, is defined as [18]:

$$\alpha = \frac{[\mathrm{W}]_\infty - [\mathrm{W}]}{[\mathrm{W}]_\infty} \quad (6)$$

where $[\mathrm{W}]_\infty$ is the catalyst ultimate capacity for the carbonaceous deposits. It has been determined experimentally for different $[\mathrm{Phenol}]_0$/[catalyst] ratios and its average value was approximately 22% C (g C g^{-1} cat.) [7].

The model-predicted data for phenol conversion and accumulated carbonaceous materials versus time are also shown in Fig. 4a and b as solid lines. Very good agreement between experimental data and predictions is achieved. The apparent activation energy for phenol CWO was found to be 65 kJ mol^{-1}. This value falls well within the range documented in the literature for phenol CWO: 48.3 kJ mol^{-1} for MnO_2/CeO_2 [19], 61 kJ mol^{-1} for CuO.ZnO.CoO/Al_2O_3 [20], and 85 kJ mol^{-1} for CuO.ZnO/Al_2O_3 and CuO/Al_2O_3 [21,22].

3.3. CWO over metal (co)promoted MnO_2/CeO_2

The amount of carbonaceous deposits building up over MnO_2/CeO_2 was unacceptably high and correspondingly the mineralization selectivity was too low for practical implementation of this catalyst. It was therefore proposed to promote the catalyst with noble metals and examine whether or not improvement of the mineralization selectivity is feasible. The promotion effect will likely consist in enhancing C–C bond rupture and simultaneously preventing extensive radical polymerization by either minimizing surface radical concentration or inhibiting propagation steps.

The performances of Pt and Ag-promoted MnO_2/CeO_2 catalysts were quantified in terms of phenol and total organic carbon conversions as well as in terms of the carbon content of the deposits. To assess the effect of promoter on total oxidation, a mineralization selectivity toward total inorganic carbon (formation of CO_2 and water) is used. This selectivity was defined as:

$$S_\mathrm{M} = 1 - \frac{[\mathrm{C_S}]}{TOC_0 - TOC} \quad (7)$$

in which $[\mathrm{C_S}]$ is the amount of deposited carbon per unit volume of solution.

Fig. 6 shows the *TOC* and phenol conversions attained after 60 min of reaction at 80°C versus platinum loading and metal-loading protocol. Both conversions decreased steadily with an increase of the noble metal loading up to 1 wt.%. Above this limit, phenol and *TOC* conversions reached plateaus at ca. 65 and 60%, respectively. The obtained results revealed no substantial differences between ion-exchanged and

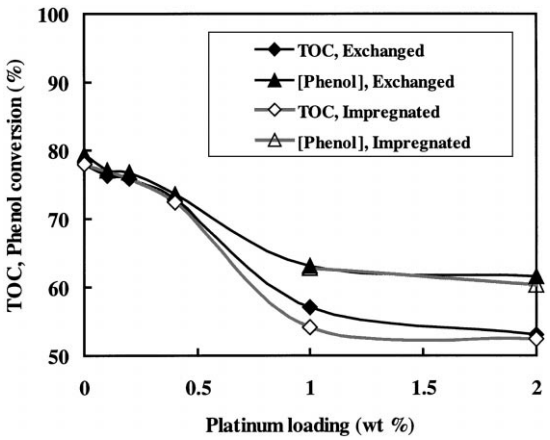

Fig. 6. Effect of metal-loading procedure and Pt loading on *TOC* and phenol conversions after 60 min of CWO at 80°C (Lines show trends).

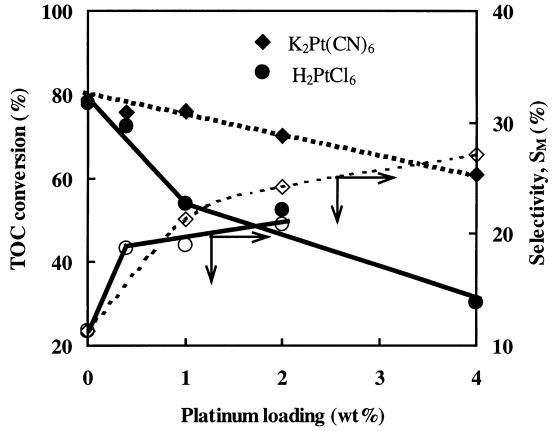

Fig. 7. *TOC* conversion and mineralization selectivity versus Pt loading on MnO_2/CeO_2 using chlorine-containing and chlorine-free Pt precursors. CWO at 60 min and 80°C (Lines show trends).

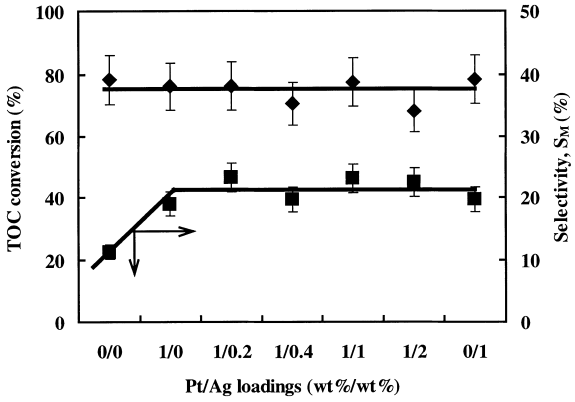

Fig. 8. *TOC* conversions and mineralization selectivity reached after 60 min of CWO at 80°C for different catalyst formulations (Lines show trends).

impregnated catalysts. In particular, irrespective of the loading procedure, phenol conversion was unaffected over the whole range of explored concentration. Whereas the *TOC* conversion seemed slightly better around 1 wt.% loadings when Pt was deposited by ion exchange.

Fig. 7 shows the *TOC* conversion and the mineralization selectivity S_M, obtained with two different Pt precursors over a range of metal loading. Even if the MnO_2/CeO_2 catalyst allowed conversions as high as 80% at 80°C, S_M barely attained 11%. Upon promotion with 0.2–0.4 wt.% Pt by ion-exchange, this selectivity was doubled. Higher *TOC* conversions were obtained with the non-chlorinated precursor, whereas S_M was virtually independent of the type of the Pt precursor. The selectivity exhibited a monotonic increase with increased metal loading and its value tripled with 4 wt.% Pt. As in Fig. 6, the *TOC* conversions diminished with increasing the metal loading, however, the loss in conversion for the non-chlorinated precursor was much less pronounced than with the chlorinated one. The lower conversions and mineralization selectivities obtained with the chlorinated Pt precursor may be explained by a higher sensitivity of the noble metal-containing oxidation catalysts to poisoning by traces of halogen-containing species remaining after the ion-exchange or impregnation of the noble metal. Although poisoning deactivation of wet oxidation catalysts by chlorine- or chloride-containing wastewaters is documented in the literature [2], this study shows that deactivation by persisting traces of halogen species from catalyst preparation is also possible.

The impact on CWO conversion and selectivity of bimetallic copromoted catalysts is illustrated in Fig. 8. In those experiments, catalysts with different silver loadings combined with only two levels of Pt loadings, i.e. 0 and 1 wt.% were tested. It can be seen that all explored bimetallic combinations lead to virtually the same *TOC* conversions and equal to that of the unpromoted manganese/cerium composite oxides. Moreover, even if there is a net gain in selectivity of the promoted catalysts compared to the unpromoted ones, all promoted catalysts performed equally. Silver alone exhibited the same performance as platinum alone and also as all bimetallic combinations. While this observation does not support the occurrence of synergism in doping the composite Mn/Ce oxide with two metals, it does show that base metals are as efficient as noble metals, and may therefore be preferred as a cost-effective option to boost the mineralization selectivity of heterogeneously-mediated wet oxidation reactions. As will be discussed in the next section, it is speculated that metal promotion is required to enhance the redox properties of the catalysts by shifting the reduction peaks to lower temperatures; the manganese oxides acting as catalytically active sites for CWO, the cerium oxides serving as oxygen storage promoters, and the metal promoting the dissociative adsorption of O_2.

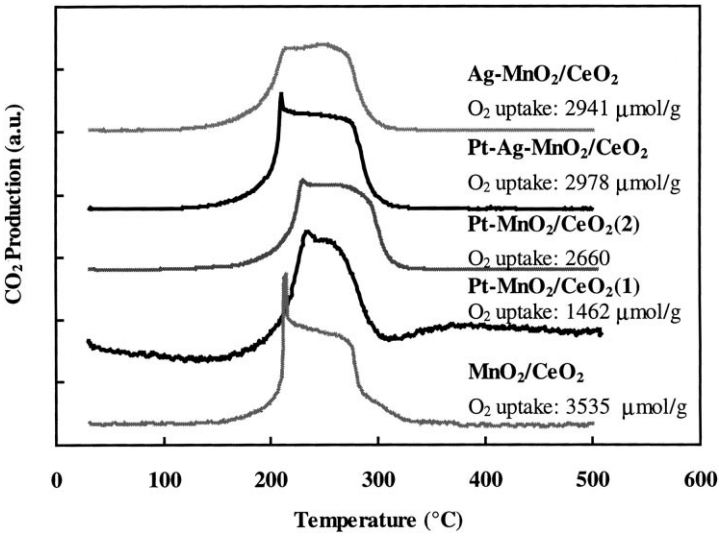

Fig. 9. TPO-MS profiles for MnO_2/CeO_2 and M–MnO_2/CeO_2 (M: Pt and/or Ag) catalysts after 60 min of CWO at 80°C (oxygen uptake is expressed in mmol g^{-1} catalyst). (1): H_2PtCl_6; (2): $K_2Pt(CN)_6$.

3.4. TPO analysis of spent catalysts

The TPO-MS technique was used to characterize the carbonaceous deposits formed on the catalysts surfaces during the wet oxidation reaction. The consumption of oxygen and formation of carbon dioxide are indicative of the amount and nature of the carbonaceous deactivating materials. Fig. 9 presents the burn-off profiles in terms of CO_2 production for the different catalyst formulations after 1 h of CWO reaction at 80°C. In the case of the unpromoted MnO_2/CeO_2 catalyst, the combustion peak exhibited two features, a sharp peak between 200 and 220°C followed by a broad one between 250 and 280°C. However, for the mono- or the bimetallic-promoted MnO_2/CeO_2, the low temperature sharp peak was no longer clearly discernible. Although the temperature window of combustion was not affected whether a metal was available or not on the composite oxide catalyst, the oxygen uptake during TPO (shown in Fig. 9) was dramatically modified by the presence of metals. Generally, oxygen uptake was much smaller with the noble metal promoted MnO_2/CeO_2 catalysts indicating that less deposits formed on the catalysts. This is also consistent with the improved mineralization selectivity of the total organic carbon (phenol and its CWO by-products) over the promoted catalysts.

4. Conclusion

The catalytic oxidation of phenol in aqueous solutions was investigated in the presence of MnO_2/CeO_2, and platinum and silver (co)promoted MnO_2/CeO_2. The CWO kinetics was described by means of a four-lump Langmuir–Hinshelwood model accounting for the occurrence of catalyst deactivation due to carbonaceous deposits on the catalyst surface. Formation of these deposits at the expense of the more desirable total oxidation product was a major drawback that was mitigated through the use of appropriate promoters. Promotion of the MnO_2/CeO_2 with Pt and/or Ag improved selectivity to fully mineralized products and maintained higher catalyst activity at very mild reaction conditions. The promoting effect of Pt and/or Ag on the MnO_2/CeO_2 catalyst was interpreted from the TPR data and ascribed to the low temperature redox properties of the MnO_2/CeO_2 attained by metal doping.

Acknowledgements

Financial support from the Natural Sciences and Engineering Research Council of Canada (NSERC) and the Fonds pour la Formation de Chercheurs et d'Aide

à la Recherche (Que.) is gratefully acknowledged. The authors wish to thank Prof. B. Grandjean for the use of the mass spectrometer.

References

[1] J. Levec, Chem. Biochem. Eng. Q. 11 (1997) 47.
[2] Y.I. Matatov-Meytal, M. Sheintuch, Ind. Eng. Chem. Res. 37 (1998) 309.
[3] V.S. Mishra, V.V. Mahajani, J.B. Joshi, Ind. Eng. Chem. Res. 34 (1995) 2.
[4] S. Imamura, Ind. Eng. Chem. Res. 38 (1999) 1743.
[5] S. Hamoudi, F. Larachi, A. Sayari, J. Catal. 177 (1998) 247.
[6] S. Hamoudi, F. Larachi, G. Cerrella, M. Cassanello, Ind. Eng. Chem. Res. 37 (1998) 3561.
[7] S. Hamoudi, K. Belkacemi, F. Larachi, Chem. Eng. Sci. 54 (1999) 3569.
[8] S. Hamoudi, F. Larachi, A. Adnot, A. Sayari, J. Catal. 185 (1999) 333.
[9] M. Luo, X. Yuan, X. Zheng, Appl. Catal. A Gen. 175 (1998) 121.
[10] L. Kundakovic, M. Flytzani-Stephanopoulos, Appl. Catal. A Gen. 183 (1999) 35.
[11] S. Imamura, M. Nakamura, N. Kawabata, J. Yoshida, S. Ishida, Ind. Eng. Chem. Prod. Res. Dev. 37 (1986) 34.
[12] S. Imamura, A. Dol, S. Ishida, Ind. Eng. Chem. Prod. Res. Dev. 24 (1985) 24.
[13] A. Trovarelli, Catal. Rev. Sci. Eng. 38 (1996) 439.
[14] M. Larsson, Coke on supported palladium and platinum catalysts. Ph.D. Thesis, Chalmers University, Götteborg, Sweden, 1997.
[15] L. Oliviero, J. Barbier Jr., S. Labruquere, D. Duprez, Catal. Lett. 60 (1999) 15.
[16] S. Kacimi, J. Barbier Jr., R. Taha, D. Duprez, Catal. Lett. 22 (1993) 343.
[17] C. De Leitenberg, D. Goi, A. Primavera, A. Trovarelli, G. Dolcetti, Appl. Catal. B Environ. 11 (1996) L29.
[18] G.F. Froment, K.B. Bischoff, Chemical Reactor Analysis and Design, Wiley, New York, 1979.
[19] Z.H. Ding, M.A. Frisch, L. Li, E.F. Gloyna, Ind. Eng. Chem. Res. 35 (1996) 3257.
[20] A. Pintar, J. Levec, Chem. Eng. Sci. 49 (1994) 4391.
[21] H. Ohta, S. Goto, H. Teshima, Ind. Eng. Chem. Fundam. 19 (1980) 180.
[22] A. Pintar, J. Levec, J. Catal. 135 (1992) 345.